Chemical Science

ROYAL SOCIETY OF CHEMISTRY

EDGE ARTICLE

View Article Online
View Journal | View Issue

Cite this: *Chem. Sci.*, 2020, **11**, 11525

All publication charges for this article have been paid for by the Royal Society of Chemistry

Received 1st July 2020
Accepted 28th September 2020

DOI: 10.1039/d0sc03627g

rsc.li/chemical-science

Fungal siderophore biosynthesis catalysed by an iterative nonribosomal peptide synthetase†

Yang Hai, ‡[a] Matthew Jenner *[bc] and Yi Tang *[ad]

Siderophores play a vital role in the viability of fungi and are essential for the virulence of many pathogenic fungal species. Despite their importance in fungal physiology and pathogenesis, the programming rule of siderophore assembly by fungal nonribosomal peptide synthetases (NRPSs) remains unresolved. Here, we report the characterization of the bimodular fungal NRPS, SidD, responsible for construction of the extracellular siderophore fusarinine C. The use of intact protein mass spectrometry, together with *in vitro* biochemical assays of native and dissected enzymes, provided snapshots of individual biosynthetic steps during NPRS catalysis. The adenylation and condensation domain of SidD can iteratively load and condense the amino acid building block *cis*-AMHO, respectively, to synthesize fusarinine C. Our study showcases the iterative programming features of fungal siderophore-producing NRPSs.

Introduction

Iron is an essential element to life, but its bioavailability is very limited owing to the poor solubility of ferric iron in aerobic environments. Hence, virtually all living organisms have evolved sophisticated mechanisms for iron acquisition and storage.[1,2] Siderophores are low-molecular-weight, high-affinity iron chelators and play a central role in maintaining iron homeostasis in bacteria, fungi, and plants.[3] Two major hydroxamate-based peptidyl siderophores are employed by fungi: the depsipeptides, exemplified by fusarinine C (FSC, **1**) and triacetylfusarinine C (TAFC, **2**),[4] and the coprogen family of siderophores (Fig. 1A).[5] These compounds are excreted primarily to capture ferric iron, assisting iron uptake. In contrast, the intracellular siderophores, represented by the ferrichrome family, are primarily used for iron storage although some fungal species have been observed to secrete such siderophores (Fig. 1A).[6] Both extra- and intracellular siderophores are indispensable for the virulence of many notorious pathogenic fungal species, such as rice blast fungus *Magnaporthe oryzae* and the human opportunistic pathogen *Aspergillus fumigatus*.[7]

Despite the preponderance of siderophores in fungal physiology and pathogenesis, the enzymes involved in fungal siderophore biosynthesis remain largely uncharacterized, in particular the core modular nonribosomal peptide synthetases (NRPS) that are essential in assembling peptidyl siderophores.[8,9] Representative examples of these NRPSs include the FSC synthetase, SidD, the coprogen synthetase, Nps6, and the ferricrocin synthetase, SidC (Fig. 1).[10–12]

Features unique to these NRPSs can be readily identified from their characteristic domain organizations. Firstly, they typically have incomplete C-terminal modules missing a functional adenylation (A) domain, which suggests the thiolation (T) domain in these modules must be aminoacylated by A domains from the upstream modules. Specifically, in both SidD and Nps6, module 2 harbours degenerate A (dA) domains which are truncated at their N-termini by nearly 290 amino acid residues and are predicted to be catalytically inactive.[13] These dA domains are likely vestiges of evolution and only play a structural role within the NRPS. In comparison, module 4 and 5 in SidC have evolved to completely lack A domains. A second defining feature is the number and order of modules in these siderophore-producing NRPSs do not match the length and sequence of their peptide siderophore products, indicating a high degree of non-colinearity.[13,14] These features distinguish them from the well-characterized fungal iterative cyclodepsipeptide (CDP) NRPSs,[15,16] all of which harbour complete modules and assemble depsipeptide antibiotics (*e.g.* enniatin) consisting of repeated dipeptide units.

To understand the molecular mechanism of this unique family of NRPSs, we focused on the elucidation of SidD-catalysed biosynthesis of FSC. Here, employing

[a]*Department of Chemical and Biomolecular Engineering, University of California, Los Angeles, California, 90095, USA. E-mail: yitang@ucla.edu*

[b]*Department of Chemistry, Warwick Integrative Synthetic Biology Center, University of Warwick, Coventry, UK. E-mail: M.Jenner@warwick.ac.uk*

[c]*Warwick Integrative Synthetic Biology (WISB) Centre, University of Warwick, Coventry, UK*

[d]*Department of Chemistry and Biochemistry, University of California, Los Angeles, California 90095, USA*

† Electronic supplementary information (ESI) available. See DOI: 10.1039/d0sc03627g

‡ Present address: Department of Chemistry and Biochemistry, University of California, Santa Barbara, Santa Barbara, California, 93106, USA.

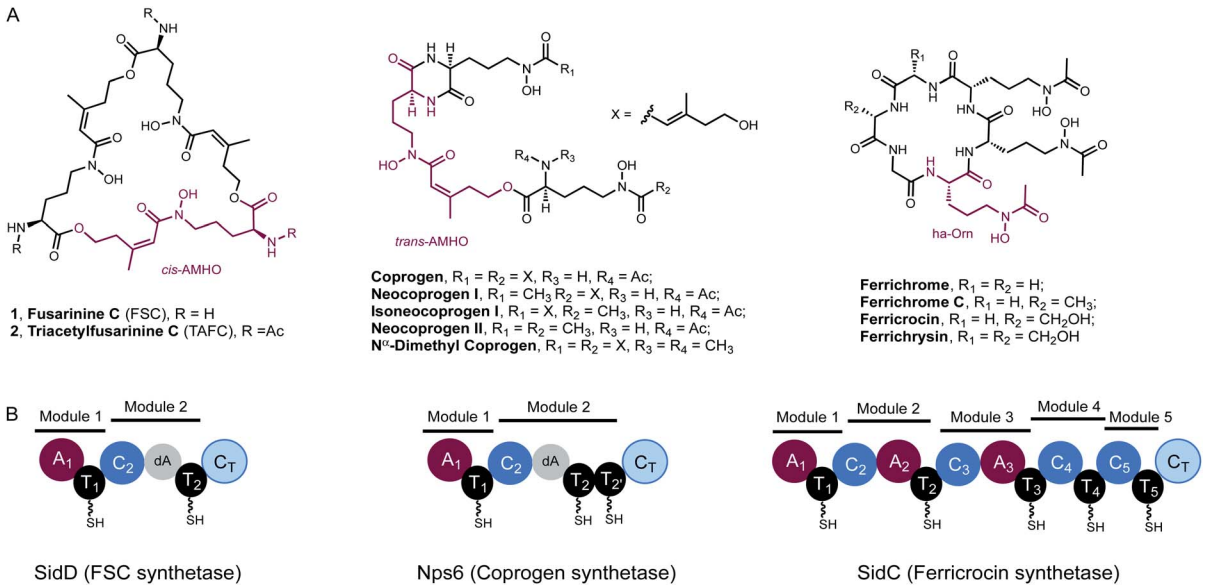

Fig. 1 Fungal hydroxamate siderophores and the domain organisation of NRPSs responsible for their biosynthesis. (A) Structures of extra- and intra-cellular siderophores shown in the desferri-form. In each case, a repeating hydroxamate unit has been highlighted in purple. TAFC and ferricrocin possess Fe^{3+} binding constants of 10^{32} and 10^{27}, respectively. (B) NRPS domain organisation of SidD, Nps6 and SidC (*left to right*). In SidD and Nps6, the dA notation represents a degenerated A domain. In SidC, module 4 and module 5 completely lack A domains.

a combination of *in vitro* biochemical assays and intact protein mass spectrometry (MS), we show how the bimodular NRPS, SidD, is precisely programmed to iteratively assemble the trimeric siderophore FSC.

Results and discussions

To decipher the mechanism of SidD, we purified recombinant SidD and its mutants (designed to dissect the domain function, *vide infra*) from *Saccharomyces cerevisiae* JHY686 strain (Fig. S1†).[17] To ensure protein samples were all in the *holo*-form, purified SidD variants were enzymatically phosphopantetheinylated using the phosphopantetheinyl transferases NpgA (*A. nidulans*) or Sfp (*B. subtilis*), as described previously.[18–21] The substrate, N^5-*cis*-anhydromevalonyl-N^5-hydroxy-L-ornithine (*cis*-AMHO) was prepared by alkaline hydrolysis of **1**.[22] We isolated **1** from an *A. nidulans* mutant in which the acetyltransferase gene *sidG* was knocked out to prevent acetylation of **1** to give **2** *in vivo* (ESI methods†).[12] In the presence of ATP and Mg^{2+}, wild-type SidD could synthesize desferri-**1** utilizing *cis*-AMHO as building blocks (Fig. 2A), while ferri-**1** was observed when Fe^{3+} was present in the substrate solution (prepared from hydrolysis of ferri-FSC without removing Fe^{3+} ions). The product identity was confirmed by comparison to a chemical standard of ferri-**1** on LC-MS (Fig. 2B). The reaction has an apparent K_M of 120 μM for *cis*-AMHO and an overall k_{cat} of 0.5 s^{-1} (Fig. 2C). Trace amounts of linear-FSC (**3**) were observed in both the authentic standard and the reaction mixture. This is likely the result of slow non-enzymatic hydrolysis of the ester bond in **1** under the assay conditions (phosphate buffer, pH 7.8), or in the reaction mixture, where additional linear-FSC (**3**) could arise from both ester hydrolysis or non-enzymatic thioester hydrolysis of the *cis*-AMHO trimer appended to the SidD protein.

Successful reconstitution of SidD activity *in vitro* allowed us to further dissect its domain function. Both thiolation (T)

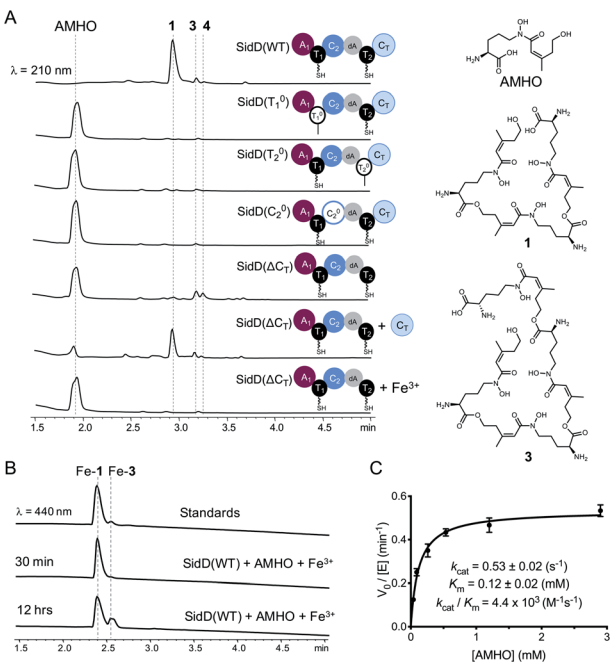

Fig. 2 Comparison of *in vitro* enzymatic assays for wild-type SidD and mutational variants. (A) HPLC traces of the enzymatic reactions for different SidD variants. The domain architectures of the variants are displayed. Mass spectral data of each peak are shown in Fig. S2–S9.† (B) Comparison of HPLC traces for the enzymatic products (in the ferri-form) with chemical standards. (C) Steady-state kinetics of wild-type SidD.

domains are essential for SidD activity, as disabling either T domain by mutating the key serine that serves as the phosphopantetheinyl group attachment site (S801A and S1594A, designated as T_1^0 and T_2^0, respectively), completely abolished FSC formation. Inactivating the condensation (C) domain from module 2 by mutating the catalytic histidine residue (H999A, designated as C_2^0) also resulted in no product formation. Interestingly, deletion of the C-terminal condensation domain (ΔC_T) yielded two shunt products: linear-FSC (**3**) and a new compound, **4**, whose molecular weight, retention time, and ability to chelate Fe^{3+} suggested a linear tetrameric derivative of FSC (Fig. 2A and S2–S9†). Addition of equimolar standalone C_T domain restored FSC synthetase activity of SidD(ΔC_T) mutant, albeit with lower efficiency compared to wild-type. These results together indicate that cyclization, but not the chain-elongation reaction, is compromised by the ΔC_T truncation mutant, whereas chain-elongation is prevented by the C_2^0 mutant. This result is consistent with the general programming rule that, C_T domains found in fungal NRPS usually offload the peptidyl products through cyclization.[23] This is in contrast to the role played by C_T domains in CDP NRPSs, which have been shown to catalyse chain elongations in addition to cyclizations.[15,16]

To obtain further insights into the function of C_2 and C_T in SidD, we prepared *cis*-AMHO-derived aminoacyl-*N*-acetylcysteamine thioester substrates and assayed individual C domain activity *in vitro*.[24] However, this approach was impeded by the instability of *cis*-AMHO and its derivatives: the *cis*-AMHO moiety is prone to degradation and yields N^5-hydroxy-L-ornithine and Δ^2-anhydro-mevalonate lactone under acidic conditions (Fig. S10†).[25,26] We therefore turned to intact protein MS to provide snapshots of SidD during the assembly of FSC. This approach has been used successfully to study the enzymology of simplified polyketide synthases (PKS) and NRPS model systems.[27–29] Here we applied this technique to capture the steps of an iterative biosynthetic assembly line.

In order to visualize enzyme-bound intermediates using intact protein MS, we chose the SidD(ΔC_T) mutant instead of wild-type SidD. Based on our previous biochemical assays (Fig. 2), this mutant assembly line is stalled without the releasing domain (C_T). This leads to accumulation of intermediates that can be captured by intact protein MS. Accordingly, *in vitro* reactions of SidD(ΔC_T) were subject to UHPLC-ESI-Q-TOF-MS analyses (Methods see ESI†). Taking *holo*-SidD(ΔC_T) as a starting point, after providing *cis*-AMHO and ATP as substrates for 15 min, we observed a new species from the deconvoluted mass spectrum (Fig. 3A). This new species corresponded to one *cis*-AMHO unit tethered to the assembly line (designated as intermediate **I**), as indicated by the mass shift of +242 Da relative to the mass of SidD(ΔC_T) in the *holo*-form. Rather than building up more intermediates, prolonged incubation (1 h) resulted in complete disappearance of intermediate **I** (Fig. 3A).

When we repeated this analysis using Fe^{3+}-containing *cis*-AMHO substrates, we observed a new species with a +1021 Da mass shift relative to *holo*-SidD(ΔC_T), corresponding to loading of four *cis*-AMHO units onto the assembly line plus a chelated ferric ion (designated as intermediate **IV**). We interpreted this

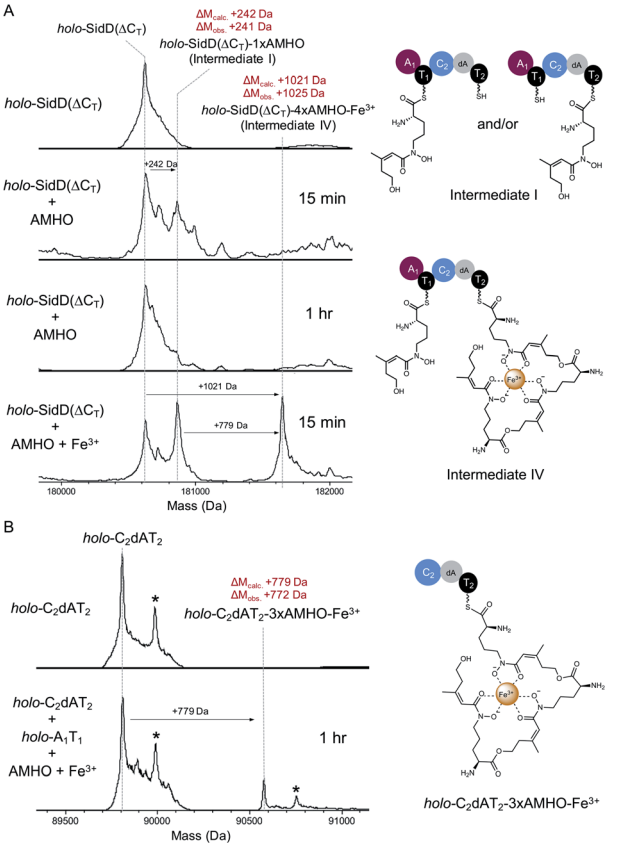

Fig. 3 Snapshots of late-stage biosynthetic intermediates. Deconvoluted intact protein mass spectra of (A) SidD(ΔC_T) mutant acting *in cis* (B) split SidD(ΔC_T) mutant (C_2dAT_2 + A_1T_1) acting *in trans*. Mass shifts corresponding to biosynthetic steps are highlighted with arrows, and proposed intermediates are displayed. Peaks labeled with asterisks indicate N-terminal gluconoylation, a known post-translational modification of recombinant heterologous proteins in *E. coli*.[11] Exact measured and observed masses are detailed in Table S5.†

intermediate as most likely T_1 charged with one *cis*-AMHO while T_2 tethered with a linear trimeric depsipeptide coordinating to a Fe^{3+} ion (Fig. 3A). However, because SidD has two phosphopantetheinyl (Ppant) arms, it is uncertain as to which T domain each proposed peptidyl intermediate is tethered and different combinations of intermediates can be envisaged (*e.g.* dimeric depsipeptides appended to both T_1 and T_2, with only one of these dimeric depsipeptide chelating the Fe^{3+} ion). To resolve this ambiguity, we performed a similar assay, using a split version of the SidD construct (A_1T_1 + C_2dAT_2) in which module 1 and module 2 must interact *in trans*, such that the mass changes on individual Ppant arm can be tracked unambiguously. As shown in Fig. 3B, a +779 Da mass shift relative to the mass of C_2dAT_2 in the *holo*-form was clearly observed for a new species corresponding to three *cis*-AMHO units attached to C_2dAT_2 plus a coordinated Fe^{3+} ion. The low population of this new species may be attributed to less efficient crosstalk between two modules acting *in trans* as compared to the intact bimodule construct. Nevertheless, this result confirmed our interpretation of intermediate **IV**, and these snapshots together strongly support our proposal that C_T domain is solely responsible for

cyclization and product release, and is not involved in chain elongation steps as seen in fungal CDP NRPSs.[15,16]

Successful trapping of the trimeric intermediate **IV** achieved only in the presence of Fe^{3+} ions indicates that shielding of the hydroxamate moieties from the oligomeric peptidyl intermediate through coordination to Fe^{3+} ion can suppress the nonenzymatic thioester cleavage leading to **3** (and **4**). Indeed, when Fe^{3+}-containing *cis*-AMHO was supplied as substrates, no product was observed in our LC-MS analysis (Fig. 2A), which is consistent with the assembly line stalled at the stage of intermediate **IV**. It is likely that in the absence of C_T domain, a nearby free hydroxamate group may act as a general base to assist direct hydrolytic cleavage of the scissile thioester bond leading to spontaneous release of the peptidyl intermediates **3** and **4**; or help cleave the thioester bond through an intramolecular displacement mechanism driven by its nucleophilicity (Fig. S11†).

Encouraged by the successful visualization of intermediate **IV**, we next applied this methodology to intercept intermediates at early stages by further inactivating T_1 and C_2 domains from the SidD(ΔC_T) mutant, respectively. When the reaction mixture of SidD(ΔC_T, C_2^0) mutant was subject to MS analysis, two species were observed (Fig. 4A). One species represents intermediate **I** while the other one has an additional mass shift of +242 Da relative to intermediate **I**, which indicates addition of totally two *cis*-AMHO units to SidD (designated as intermediate **II**).

Since no dipeptidyl-shunt products were observed in our *in vitro* assays, intermediate **II** was best interpreted as one *cis*-AMHO unit tethered on each T domain. This interpretation is also consistent with the proposed role of C_2; namely that it C_2 carries out chain-elongation reactions. When the assay mixture of SidD(ΔC_T, T_1^0) mutant was analysed, only one major species corresponding to one *cis*-AMHO unit tethered was observed (Fig. 4B). Since now only T_2 has the obligatory Ppant arm for substrate tethering, this covalently-bound monomeric *cis*-AMHO unit must be attached to T_2 (intermediate **I′**). This result also unambiguously proves that direct intermodular substrate loading between A_1 and T_2 has occurred and bypassed T_1. Thus, the queuing model hypothesis, in which loading of T_2 is T_1-dependent (activated *cis*-AMHO substrate is transferred from T_1 to T_2 through transthioesterification), can be ruled out (Fig. S12†).

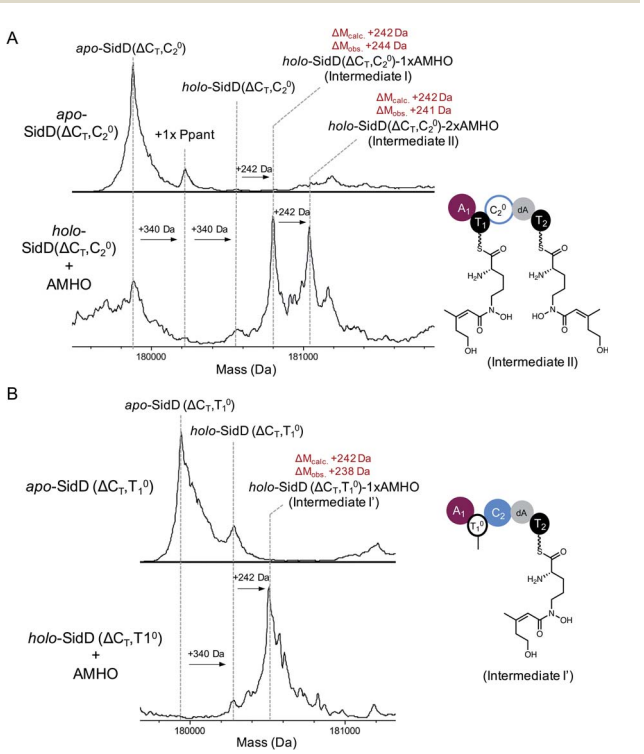

Fig. 4 Snapshots of early-stage biosynthetic intermediates. Deconvoluted intact protein mass spectra of (A) SidD(ΔC_T, C_2^0) mutant and (B) SidD(ΔC_T, T_1^0) mutant. Exact measured and observed masses are detailed in Table S5.†

Taken together, we propose a working model for SidD (Fig. 5). The only functional A domain from module 1 (A_1) must aminoacylate T domains from both modules. However, whether loading of each module is in an ordered or random sequence remains unresolved. Once both T domains are charged with *cis*-AMHO, chain elongation will be catalysed by C_2 to give a dimeric *cis*-AMHO intermediate (tethered to T_2). Meanwhile, the vacant T_1 will be charged with another *cis*-AMHO unit by A_1. The C_T domain is likely to dictate the chain-length by favouring a 36-membered ring closure cyclization reaction on a trimeric intermediate bound on T_2. Similar chain-length determining role of C_T has been proposed in CDP NRPSs.[15,16] Hence, if the dimer intermediate reaches C_T, it will be rejected and return to C_2 to condense another *cis*-AMHO unit from T_1, yielding the desired on-pathway trimer intermediate that can be offloaded by C_T through cyclization to yield FSC (**1**). It is noteworthy that in this biosynthetic model, the C_2 domain must accommodate substrates of different chain lengths appended to T_2 for each of the condensation events (*i.e.* monomeric *cis*-AMHO *vs.* dimeric *cis*-AMHO). Although this scenario would require the C_2 domain to catalyse chain elongation using different acyl-acceptors, *i.e.* the terminal hydroxyl moiety from substrates of vastly different chain lengths (12-membered *vs.* 24-membered), similar iterative use of C domain has been proposed for asperlicin biosynthesis.[30]

Our proposed working model could also explain the formation of shunt products **3** and **4**. In the absence of C_T, the SidD assembly line will progress and stall when the trimer intermediate is reached. Hydroxamate-assisted, slow non-enzymatic thioester cleavage will occur, eventually releasing the stalled intermediate as shunt product **3**. Furthermore, the long-lived trimer intermediate could now have a chance to complete an aberrant chain-elongation reaction presumably at C_2 with a rate comparable to that of the hydrolytic releasing of **3**, which could explain the formation of derailed product **4** (Fig. S13†). Formation of the longer-than-desired product **4** in the absence of C_T further reinforced the idea that C_T, rather than C_2 is the chain-length determining domain. Offloading either **3** or **4** will free up T_2 and enable multiple turnovers of the substrate.

A subtle variation on this pathway could also be envisioned, in which the dimeric *cis*-AMHO intermediate bound to T_2 following the first condensation event is "back transferred" onto T_1 *via* a *trans*-thioesterification step, followed by loading of

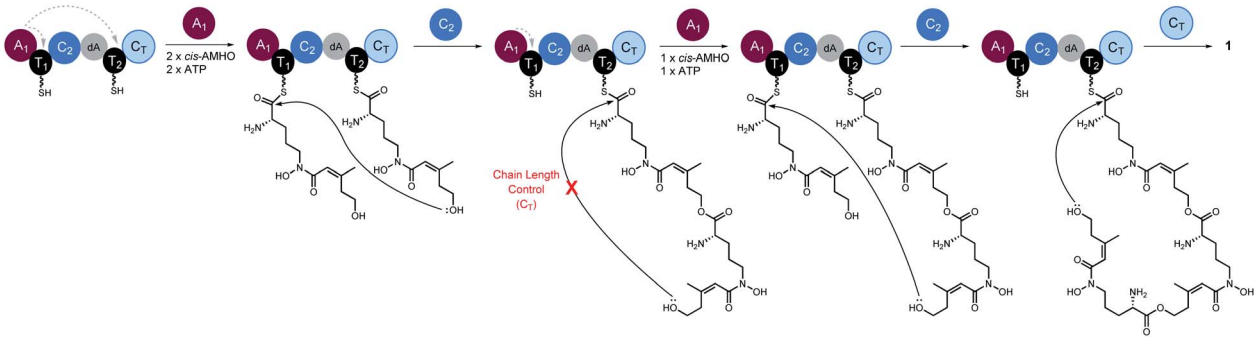

Fig. 5 Proposed biosynthetic model for SidD-catalysed formation of FSC (**1**). Grey dashed arrows indicate productive interactions between the A_1 domains and the T_1/T_2 domains. Our data suggest that the C_T domain, not the central C_2 domain, determines the chain-length of the nascent peptidyl chain permitted for cyclisation. A subtle variation of this model involving a chain back-transfer step cannot be ruled out and is outlined in Fig. S13.†

T_2 with another *cis*-AMHO unit. This would mean that C_2 always utilises monomeric *cis*-AMHO from the T_2 domain (Fig. S14†). Although such "chain back-transfer" step cannot be ruled out by our current data, it is unprecedented for NRPS enzymology. It is worth noting, that although "pass-back chain extension" has been observed in fungal CDP NRPSs and bacterial PKS–NRPS hybrids,[15,31] it is different from the "chain back-transfer" proposed here. The aforementioned, "chain back-transfer" does not involve chain elongation, whilst "pass-back chain extension" is essentially a chain elongation step except the direction is not forward. This difference also renders SidD distinct from the closely related CDP NRPSs. The C_T domains from CDP NRPSs not only catalyze chain cyclization to offload the final cyclicdepsipeptides, but also catalyses "pass-back chain extension" to enable iterative use of the whole assembly line; whereas the C_T domain from SidD is solely involved in cyclization since elongated products are still observed in the absence of C_T.

Our mechanistic study of SidD also provides valuable insights into the biosynthesis of other fungal siderophores, in particular, the coprogen-type siderophores. Nps6 shares several striking similarities with SidD: (1) they adopt almost identical domain architectures (except in Nps6 tandem repeated T domains are present in module 2; and (2) they utilize very similar building blocks (SidD activates *cis*-AMHO while NPS6 activates *trans*-AMHO), yet they make distinct products: coprogen is a partially linear depsipeptide while FSC is a *bona fide* macrocycle. Based on our study of SidD, we expect that Nps6 should iteratively use A_1 to aminoacylate T domains in both of its modules (*i.e.* three T domains in total). The tandem T domains in Nps6 module 2 are likely employed to increase overall flux.[32] Assuming the C_T domain in Nps6 also catalyses cyclization and chain release to forge the diketopiperazine scaffold, then the C_2 domain must be iteratively used to account for the extra chain elongation in this bimodular NRPS. Intriguingly, if this proposal is correct, the C_2 domain from Nps6 would be a C domain with dual-function; catalysing both ester bond and amide bond formation. We hypothesise that when the Nps6 C_2 domain catalyses a second chain elongation event, it attaches T_1-tethered *trans*-AMHO to the amino group of T_2-tethered *trans*-AMHO dimers instead of the hydroxy group at the end of the growing chain as proposed for the SidD C_2 domain. Then a C_T-catalysed intra-molecular cyclisation would simultaneously yield the diketopiperazine moiety and release the coporgen product from the NRPS (Fig. S15†). Although this biosynthetic proposal is consistent with our working model for SidD, the exact molecular mechanism of Nps6 undoubtedly warrants more in-depth biochemical investigation in the future.

Conclusions

We have provided evidence supporting an iterative NRPS mechanism for SidD, including an iterative A domain, iterative chain-elongation C domain, and a chain-releasing C_T domain catalysing cyclization and determining product chain-length, respectively. The iterative use of A domains to incorporate repeat units of hydroxamate amino acids is a hallmark for fungal siderophore-producing NRPS and a remarkable strategy to improve atom economy for biosynthetic assembly-lines. Understanding the molecular mechanism underpinning such programmed and highly efficient iterative domain usage may guide future design and engineering of novel and smaller NRPS assembly-lines.

Conflicts of interest

There are no conflicts to declare.

Acknowledgements

This work was supported by the NIH 1R35GM118056 to YT. YH is a Life Sciences Research Foundation fellow sponsored by the Mark Foundation for Cancer Research. M. J. is the recipient of a BBSRC Future Leader Fellowship (BB/R01212/1). The Bruker MaXis II instrument used in this study was funded by the BBSRC (BB/M017982/1).

Notes and references

1 C. D. Kaplan and J. Kaplan, *Chem. Rev.*, 2009, **109**, 4536–4552.

2 S. C. Andrews, A. K. Robinson and F. Rodríguez-Quiñones, *FEMS Microbiol. Rev.*, 2003, **27**, 215–237.
3 M. Miethke and M. A. Marahiel, *Microbiol. Mol. Biol. Rev.*, 2007, **71**, 413–451.
4 A. H. T. Hissen and M. M. Moore, *J. Biol. Inorg Chem.*, 2005, **10**, 211–220.
5 H. Haas, *Nat. Prod. Rep.*, 2014, **31**, 1266–1276.
6 A. C. W. Franken, B. E. Lechner, E. R. Werner, H. Haas, B. C. Lokman, A. F. J. Ram, C. A. M. J. J. van den Hondel, S. de Weert and P. J. Punt, *Brief. Funct. Genomics*, 2014, **13**, 482–492.
7 H. Haas, M. Eisendle and B. G. Turgeon, *Annu. Rev. Phytopathol.*, 2008, **46**, 149–187.
8 T. Schwecke, K. Göttling, P. Durek, I. Dueñas, N. F. Käufer, S. Zock-Emmenthal, E. Staub, T. Neuhof, R. Dieckmann and H. von Döhren, *ChemBioChem*, 2006, **7**, 612–622.
9 K. E. Bushley, D. R. Ripoll and B. G. Turgeon, *BMC Evol. Biol.*, 2008, **8**, 328.
10 S. Oide, W. Moeder, S. Krasnoff, D. Gibson, H. Haas, K. Yoshioka and B. G. Turgeon, *Plant Cell*, 2006, **18**, 2836–2853.
11 K. Reiber, E. P. Reeves, C. M. Neville, R. Winkler, P. Gebhardt, K. Kavanagh and S. Doyle, *FEMS Microbiol. Lett.*, 2005, **248**, 83–91.
12 M. Schrettl, E. Bignell, C. Kragl, Y. Sabiha, O. Loss, M. Eisendle, A. Wallner, H. N. Arst, K. Haynes and H. Haas, *PLoS Pathog.*, 2007, **3**, 1195–1207.
13 H. D. Mootz, D. Schwarzer and M. A. Marahiel, *ChemBioChem*, 2002, **3**, 490–504.
14 R. D. Süssmuth and A. Mainz, *Angew. Chemie. Int. Ed.*, 2017, **56**, 3770–3821.
15 D. Yu, F. Xu, S. Zhang and J. Zhan, *Nat. Commun.*, 2017, **8**, 1–11.
16 C. Steiniger, S. Hoffmann, A. Mainz, M. Kaiser, K. Voigt, V. Meyer and R. D. Süssmuth, *Chem. Sci.*, 2017, **8**, 7834–7843.
17 C. J. B. Harvey, M. Tang, U. Schlecht, J. Horecka, C. R. Fischer, H. C. Lin, J. Li, B. Naughton, J. Cherry, M. Miranda, Y. F. Li, A. M. Chu, J. R. Hennessy, G. A. Vandova, D. Inglis, R. S. Aiyar, L. M. Steinmetz, R. W. Davis, M. H. Medema, E. Sattely, C. Khosla, R. P. S. Onge, Y. Tang and M. E. Hillenmeyer, *Sci. Adv.*, 2018, **4**, eaar5459.
18 H. Oberegger, M. Eisendle, M. Schrettl, S. Graessle and H. Haas, *Curr. Genet.*, 2003, **44**, 211–215.
19 Y. Hai, A. M. Huang and Y. Tang, *Proc. Natl. Acad. Sci. U. S. A.*, 2019, **116**, 10348–10353.
20 Y. Hai, M. Jenner and Y. Tang, *J. Am. Chem. Soc.*, 2019, **141**, 16222–16226.
21 L. E. N. Quadri, P. H. Weinreb, M. Lei, M. M. Nakano, P. Zuber and C. T. Walsh, *Biochemistry*, 1998, **37**, 1585–1595.
22 E. Brandenburger, M. Gressler, R. Leonhardt, G. Lackner, A. Habel, C. Hertweck, M. Brock and D. Hoffmeister, *Appl. Environ. Microbiol.*, 2017, **83**, e01478-17.
23 X. Gao, S. W. Haynes, B. D. Ames, P. Wang, L. P. Vien, C. T. Walsh and Y. Tang, *Nat. Chem. Biol.*, 2012, **8**, 823–830.
24 D. E. Ehmann, J. W. Trauger, T. Stachelhaus and C. T. Walsh, *Chem. Biol.*, 2000, **7**, 765–772.
25 H. Diekmann and H. Zahner, *Eur. J. Biochem.*, 1967, **3**, 213–218.
26 A. Munawar, J. W. Marshall, R. J. Cox, A. M. Bailey and C. M. Lazarus, *ChemBioChem*, 2013, **14**, 388–394.
27 A. von Tesmar, M. Hoffmann, J. Pippel, A. A. Fayad, S. Dausend-Werner, A. Bauer, W. Blankenfeldt and R. Müller, *Cell Chem. Biol.*, 2017, **24**, 1216–1227.e8.
28 M. Jenner, X. Jian, Y. Dashti, J. Masschelein, C. Hobson, D. M. Roberts, C. Jones, S. Harris, J. Parkhill, H. A. Raja, N. H. Oberlies, C. J. Pearce, E. Mahenthiralingam and G. L. Challis, *Chem. Sci.*, 2019, **10**, 5489–5494.
29 J. Masschelein, P. K. Sydor, C. Hobson, R. Howe, C. Jones, D. M. Roberts, Z. Ling Yap, J. Parkhill, E. Mahenthiralingam and G. L. Challis, *Nat. Chem.*, 2019, **11**, 906–912.
30 X. Gao, W. Jiang, G. Jiménez-Osés, M. S. Choi, K. N. HouK, Y. Tang and C. T. Walsh, *Chem. Biol.*, 2013, **20**, 870–878.
31 J. J. Zhang, X. Tang, T. Huan, A. C. Ross and B. S. Moore, *Nat. Chem. Biol.*, 2020, **16**, 42–49.
32 J. Crosby and M. P. Crump, *Nat. Prod. Rep.*, 2012, **29**, 1111–1137.

